Inclusive hadron production in photon-photon collisions at next-to-leading order

J. Binnewies,[1] B. A. Kniehl,[2] and G. Kramer[1]
[1]*II. Institut für Theoretische Physik, Universität Hamburg, Luruper Chaussee 149, 22761 Hamburg, Germany*
[2]*Max-Planck-Institut für Physik, Werner-Heisenberg-Institut, Föhringer Ring 6, 80805 Munich, Germany*
(Received 15 January 1996)

We study inclusive charged-hadron production in collisions of quasireal photons at next-to-leading order (NLO) in the QCD-improved parton model, using fragmentation functions recently extracted from PEP and LEP1 data of e^+e^- annihilation. We consistently superimpose the direct (DD), single-resolved (DR), and double-resolved (RR) $\gamma\gamma$ channels. We consider photon spectra generated by electromagnetic bremsstrahlung and/or beamstrahlung off colliding e^+ and e^- beams as well as those which result from backscattering of laser light off such beams. First, we reconsider existing single-tag data taken by TASSO at PETRA and by MARK II at PEP (with e^+e^- energy $\sqrt{s}\approx 30$ GeV) and confront them with our NLO calculations imposing the respective experimental cuts. We also make comparisons with the neutral-kaon to charged-hadron ratio measured by MARK II. Then, we present NLO predictions for LEP2, a next-generation e^+e^- linear collider (NLC) in the TESLA design with $\sqrt{s}=500$ GeV, and a Compton collider obtained by converting a 500-GeV NLC. We analyze transverse-momentum and rapidity spectra with regard to the scale dependence, the interplay of the DD, DR, and RR components, the sensitivity to the gluon density inside the resolved photon, and the influence of gluon fragmentation. It turns out that the inclusive measurement of small-p_T hadrons at a Compton collider would greatly constrain the gluon density of the photon and the gluon fragmentation function. [S0556-2821(96)01711-0]

PACS number(s): 13.65.+i, 13.60.Hb, 13.60.Le, 13.87.Fh

I. INTRODUCTION

The inclusive production of single hadrons in fixed-target and colliding-beam experiments has been one of the most important testing grounds for the QCD-improved parton model. In contrast to the collective observation of jets of hadrons, the detection of single mesons and baryons also allows one to study fragmentation, i.e., the mechanism of how partons (quarks, gluons, and photons) turn into hadronic matter. In the framework of the QCD-improved parton model, the cross section of inclusive single-hadron production is described as a convolution of the parton-parton scattering cross sections with the parton density functions (PDF's) of the initial-state particles and the fragmentation functions (FF's), which characterize the transition of the partons that come out of the hard scattering to the hadrons that finally hit the detector. The factorization theorem [1] ensures that the PDF's and FF's are universal and that only the partonic cross sections change when different processes are considered. While the partonic cross sections may be perturbatively calculated from the QCD Lagrangian, this is not yet possible for the PDF's and the FF's of hadrons with masses smaller than or comparable to the asymptotic scale parameter Λ, and one has to determine them by fitting experimental data. The PDF's of protons and photons, which are needed to describe, e.g., $p\bar{p}$, ep, and $\gamma\gamma$ reactions, are already highly constrained by measurements of deep inelastic ep and $e\gamma$ processes.

The most direct way to obtain information on the FF's of hadrons is to analyze their energy spectrum measured in e^+e^- annihilation, where the theoretical predictions are not obscured by additional nonperturbative input, e.g., in the form of PDF's for the incoming particles. After the extraction of leading-order (LO) FF's for pions and kaons from low-energy data of e^+e^- annihilation and muon-nucleon deep inelastic scattering in the late 1970s and early 1980s [2], there had long been no progress in this field. Some time ago, new next-to-leading-order (NLO) FF sets for charged and neutral pions and kaons as well as for η mesons were fitted to e^+e^- data generated with well-established Monte Carlo (MC) programs, which are fine-tuned so as to describe well a broad selection of experimental data [3]. An alternative approach is to directly fit to experimental data. We took this avenue for charged pions and kaons [4,5] and neutral kaons [6] by analyzing SLAC PEP and recent CERN LEP1 data. The assumption that the s, c, and b (d, c, and b) quarks fragment into charged pions (kaons) in the same way, which we had to make in Ref. [4], could be discarded in Ref. [5], thanks to the advent of accurate data from the ALEPH Collaboration at LEP1 [7], in which the fragmentation of gluons, b quarks, and light flavors into charged hadrons was distinguished. In the meantime, these data have become available in published form [8], where the fragmentation of quarks into charged hadrons is also reported for an enriched c-quark sample. This latter information was not at our disposal at the time of our analysis [5]. However, we verified that our c-quark FF's for charged hadrons are approximately in agreement with this new measurement. In order to probe the scaling violation predicted by the Altarelli-Parisi equations [9], we made comparisons with other e^+e^- data collected at different center-of-mass (c.m.) energies. To test the validity of the factorization theorem for fragmentation, we also confronted measurements of inclusive single-hadron production by the H1 [10] and ZEUS [11] Collaborations at the DESY ep collider HERA and by the UA1 Collaboration [12] at the CERN $Sp\bar{p}S$ collider with the corresponding theoretical predictions based on our FF's [5,6,13].[1] In all cases, we found good agreement. Existing data on inclusive

single-hadron production in collisions of quasireal photons offer yet another opportunity to quantitatively check the factorization theorem, which we wish to seize in the following.

The purpose of this work is to use our new FF's for charged pions and kaons [5] to make predictions for inclusive single-charged-particle production in $\gamma\gamma$ collisions, which can soon be confronted with the first experimental data from LEP2. With the exception of inclusive π^0 production [14], there exist no NLO predictions for inclusive particle production at LEP2 in the literature. We also consider $\gamma\gamma$ physics at a next-generation e^+e^- linear collider (NLC) with c.m. energy $\sqrt{s}=500$ GeV. Furthermore, we compare our NLO analysis with $\gamma\gamma$ data at low c.m. energies measured some time ago with the TASSO detector at DESY PETRA [15] and with the MARK II detector at SLAC PEP [16]. These data are at rather low p_T, where our NLO formalism is not expected to yield reliable results, so that a meaningful test of our FF's may not be possible.

As is well known, three mechanisms contribute to the production of quarks and gluons in $\gamma\gamma$ collisions: (i) In the production through direct photons (DD), the two photons directly couple to the quark lines in the hard-scattering amplitudes. At least to LO, no spectator particles travel along the photon axes. (ii) If one of the photons splits into a flux of quarks (and gluons), one of these quarks may directly interact with the second photon. The remaining quarks (and gluons) build up a spectator jet in the direction of the split photon [single-resolved (DR) γ contribution]. The $\gamma\gamma$ cross section of this mechanism depends on the PDF's of the photon. (iii) If both photons split into quarks and gluons [double-resolved (RR) γ contribution], two spectator jets appear. Since the PDF's of the photon take large values—at small x through the gluon part and at large x through the so-called pointlike quark part—the DR and RR contributions are numerically of the same order as the DD one. We perform a consistent NLO analysis, i.e., we include the DD, DR, and RR hard-scattering cross sections, the photon PDF's, and the FF's at NLO.

The outline of this work is as follows. In Sec. II, we briefly describe the formalism which we use to calculate the DD, DR, and RR contributions up to NLO. Section III contains our numerical results for PETRA, PEP, LEP2, and NLC energies. Here, we also compare with the TASSO and MARK II data. Our conclusions are summarized in Sec. IV.

II. FORMALISM

When we speak of $\gamma\gamma$ collisions with almost real photons, we have in mind the e^+e^--collision process where the positrons and electrons act as sources of nearly massless, collinear photons, which collide with each other to produce a debris of hadrons in the final state. The energy spectrum for the produced photons is well described by the equivalent-photon approximation (EPA). In this approximation, the longitudinal- and transverse-momentum components decouple. The transverse momentum is integrated out with certain constraints, specified by the experimental situation. The resulting spectra for the photons emitted from the positrons and electrons are thus functions of the longitudinal-momentum fractions, x_1 and x_2, respectively. These distributions depend on the experimental setup. In our analysis, we consider past and future experiments at the colliders PETRA, PEP, LEP2, and NLC (TESLA design or laser spectrum). The respective forms of the EPA will be specified later when we present our numerical results.

Our notation is as follows. We consider the reaction

$$e^+(p_1)+e^-(p_2)\to e^+(p_1')+e^-(p_2')+h(p_h)+X, \quad (1)$$

where h is the observed hadron and X includes all unobserved hadrons. The four momentum assignments are indicated in the parentheses. In the EPA, the inclusive cross section of process (1) is related to that of the corresponding $\gamma\gamma$ reaction,

$$\gamma_1(p_1^\gamma)+\gamma_2(p_2^\gamma)\to h(p_h)+X, \quad (2)$$

through

$$E_h\frac{d^3\sigma(e^+e^-\to e^+e^-h+X)}{d^3p_h} = \int_{x_1^{\min}}^1 dx_1\int_{x_2^{\min}}^1 dx_2 F_{\gamma_1/e^+}(x_1)F_{\gamma_2/e^-}(x_2) \times E_h\frac{d^3\sigma(\gamma_1\gamma_2\to h+X)}{d^3p_h}, \quad (3)$$

where $x_i=E_i^\gamma/E_i$ $(i=1,2)$ and $F_{\gamma_i/e^\pm}(x_i)$ stand for the photon-spectrum functions to be specified later on. The lower bounds of integration, $x_{1,2}^{\min}$, are fixed by kinematics in terms of the transverse momentum p_T and c.m. rapidity y of h. In the applications to follow, the actual e^+ and e^- acceptances must be incorporated in the integration ranges of x_1 and x_2, respectively.

In the QCD-improved parton model, the cross section of reaction (2) is expressed as a convolution of the parton-parton scattering cross sections, where one or both of the incoming partons may be photons, with the scale-dependent PDF's and FF's,

$$\begin{aligned}E_h\frac{d^3\sigma(\gamma_1\gamma_2\to h+X)}{d^3p_h} &= \int\frac{dx_h}{x_h^2}\sum_c D_{h/c}(x_h,M_h^2)\Bigg[p_c^0\frac{d^3\sigma(\gamma_1\gamma_2\to c+X)}{d^3p_c} \\ &+\sum_a\int dx_a F_{a/\gamma}(x_a,M_\gamma^2)p_c^0\frac{d^3\sigma(a\gamma_2\to c+X)}{d^3p_c} \\ &+\sum_b\int dx_b F_{b/\gamma}(x_b,M_\gamma^2)p_c^0\frac{d^3\sigma(\gamma_1 b\to c+X)}{d^3p_c} \\ &+\sum_{a,b}\int dx_a F_{a/\gamma}(x_a,M_\gamma^2)\int dx_b F_{b/\gamma}(x_b,M_\gamma^2) \\ &\times p_c^0\frac{d^3\sigma(ab\to c+X)}{d^3p_c}\Bigg]. \end{aligned} \quad (4)$$

[1]The NLO results shown in Ref. [12] were taken from Ref. [13], where the FF's of Ref. [4] were employed.

Here, the parton indices a,b,c run over the gluon and N_F flavors of quarks and antiquarks, $k_a=x_a p_1^\gamma$, $k_b=x_b p_2^\gamma$, and $k_c=p_h/x_h$ are the parton momenta, $F_{a/\gamma}(x_a,M_\gamma^2)$ is the PDF of parton a inside the photon, and $D_{h/c}(x_h,M_h^2)$ is the FF of parton c into hadron h. The factorization scales, M_γ and M_h, will be specified later on. The first term on the right-hand side of Eq. (4) is the direct-photon contribution (DD), the second and third ones are the once-resolved contributions (DR), and the fourth one is the twice-resolved contribution (RR). In LO, the DD contribution is of $O(\alpha^2)$, where α is the electromagnetic coupling constant, i.e., it is of the same order as the the respective hard-scattering cross sections. The LO hard-scattering cross sections in the DR and RR components are of $O(\alpha\alpha_S)$ and $O(\alpha_S^2)$, respectively, so that, at first sight, the LO DR and RR contributions might be considered to be of higher orders in the strong coupling constant, α_S. However, they are formally and numerically of the same order as the LO direct part, since the quark PDF's of the photon are enhanced by the factor α/α_S and the gluon PDF is enhanced at small x [17]. In fact, the factor α/α_S from the photon PDF's properly adjusts the orders of the DR and RR contributions.

It is convenient to define PDF's for finding a particular parton a, with momentum fraction x, inside the positron or electron, $F_{a/e^\pm}(x,M^2)$. In the EPA, this function is given by the convolution of the respective photon PDF, $F_{a/\gamma}(x,M^2)$, with the photon-spectrum function, $F_{\gamma/e^\pm}(x)$, introduced in Eq. (3), viz.,

$$F_{a/e^\pm}(x,M^2)=\int_x^1\frac{dy}{y}F_{a/\gamma}\left(\frac{x}{y},M^2\right)F_{\gamma/e^\pm}(y). \tag{5}$$

If the photon directly participates in the hard scattering, the photon PDF in Eq. (5) must be replaced by the delta function $\delta(1-x/y)$. Using definition (5), we can combine Eqs. (3) and (4) in one formula. The inclusive cross section to NLO is then written as

$$\begin{aligned}E_h\frac{d^3\sigma(e^+e^-\to e^+e^-h+X)}{d^3p_h}&=\sum_{a,b,c}\int dx_1dx_2\frac{dx_h}{x_h^2}F_{a/e^\pm}(x_1,M_\gamma^2)F_{b/e^\pm}(x_2,M_\gamma^2)\\&\times D_{h/c}(x_h,M_h^2)\frac{1}{\pi s}\left[\frac{1}{v}\frac{d\sigma^0_{k_ak_b\to k_c}}{dv}(s,v;\mu^2)\delta(1-w)\right.\\&\left.+\frac{\alpha_S(\mu^2)}{2\pi}K_{k_ak_b\to k_c}(s,v,w;\mu^2,M_\gamma^2,M_h^2)\right],\end{aligned} \tag{6}$$

where it is understood that the QCD-corrected hard-scattering cross sections in the DD, RR, and two DR channels are properly multiplied with the respective e^+ and e^- PDF's and summed over. As usual, $v=1+t/s$ and $w=-u/(s+t)$, where $s=(k_a+k_b)^2$, $t=(k_a-k_c)^2$, and $u=(k_b-k_c)^2$ are the Mandelstam variables at the parton level. They are related to the external Mandelstam variables, $S=(p_1+p_2)^2$, $T=(p_1-p_2)^2$, and $U=(p_2-p_h)^2$, by $s=x_1x_2S$, $t=x_1T/x_h$, and $u=x_2U/x_h$. The functions $K_{k_ak_b\to k_c}(s,v,w;\mu^2,M_\gamma^2,M_h^2)$ contain the NLO corrections to the hard-scattering cross sections, and μ is the QCD renormalization scale.

The $K_{k_ak_b\to k_c}$ functions for the DD channel have been derived by Aurenche *et al.* [18] and have recently been confirmed by Gordon [14]. The DR $K_{k_ak_b\to k_c}$ functions have been calculated in Ref. [19] and reevaluated in Ref. [14], where explicit expressions may be found. The RR $K_{k_ak_b\to k_c}$ functions have been obtained in Ref. [20]. They have recently been applied to predict single-charged-particle production in low-Q^2 ep scattering [21]. Direct and resolved photoproduction in ep scattering correspond to the DR and RR components in $\gamma\gamma$ scattering, and we may convert our previous analysis by replacing the proton PDF's with the photon PDF's. For the evaluation of the DD contribution, we employ a computer code created by Gordon in connection with Ref. [14].

For consistency, one needs both the photon PDF's and FF's in NLO. As photon PDF's we use the NLO set by Glück, Reya, and Vogt (GRV) [22], which we translate into the $\overline{\rm MS}$ factorization scheme. In their analysis, the M_γ^2 evolution starts at a rather low value, $M_0^2=0.3\ {\rm GeV}^2$. Therefore this set is also applicable at rather small p_T. However, one should keep in mind that the predictions may not be reliable in the small-p_T region because α_S is large and nonperturbative effects may dominate. As FF's for charged particles, i.e., the sum of charged pions and kaons, we employ our recently constructed NLO set [5], which has been extracted in the $\overline{\rm MS}$ factorization scheme. This scheme has also been employed for the derivation of the NLO kernels $K_{k_ak_b\to k_c}$.

In the calculation of the $K_{k_ak_b\to k_c}$ functions pertinent to the DD and DR channels, one encounters collinear singularities associated with the splitting of the incoming photons into $q\overline{q}$ pairs. These initial-state singularities are absorbed into the bare PDF's appearing in the resolved-photon contributions, i.e., the DR and RR components, which renders these functions M_γ dependent. A similar M_γ dependence, but with opposite sign, shows up in the $K_{k_ak_b\to k_c}$ functions of the DD and DR processes. In this way, the DD, DR, and RR processes become interrelated. The DR (RR) part is actually a NLO contribution to the DD (DR) part that cannot be treated fully perturbatively anymore. This nonperturbative part is then described by the photon PDF's. Up to higher-order terms in the photon PDF's, the M_γ dependence cancels in the combination of the DD and DR contributions on one hand, and the DR and RR contributions on the other hand. It is clear that the classification into DD, DR, and RR contributions becomes ambiguous if NLO corrections are included. NLO terms that have been attributed to the DD (DR) contribution may be shifted to the DR (RR) part. The cancellation of the dependences on M_γ and the choice of factorization scheme associated with the incoming-photon leg in the superposition of direct and resolved photoproduction in ep scattering have been demonstrated in Ref. [21]. We expect that this cancellation also works for the $\gamma\gamma$ process (2). The formal aspects of such cancellations in $\gamma\gamma$ reactions have been investigated by Gordon [14].

III. NUMERICAL RESULTS

We are now in a position to present our numerical results for the cross section of inclusive charged-particle production in $\gamma\gamma$ collisions at NLO. Our plan is as follows. First, we consider existing data taken at low energies by TASSO [15] and MARK II [16] and confront them with the corresponding NLO calculations. Then, we make predictions for LEP2 and NLC, superimposing the energy spectra of the usual EPA bremsstrahlung off the incoming positrons and electrons and of beamstrahlung according to the TESLA design to be discussed later. As a further application, we consider $\gamma\gamma$ collisions with photon spectra as they result from Compton backscattering of laser light off the e^+ and e^- beams of the NLC. If this method works, it will be possible to generate high-luminosity beams of real photons carrying approximately 80% of the e^+ (e^-) energy (see Ref. [23] for the impact of various NLC collider options).

We work in the $\overline{\text{MS}}$ renormalization and factorization scheme with $N_F=5$ active quark flavours and $\Lambda^{(5)}_{\overline{\text{MS}}}=131$ MeV, except for our TASSO and MARK II analyses, where we use $N_F=4$ and $\Lambda^{(4)}_{\overline{\text{MS}}}=200$ MeV. We identify the various scales and set $\mu=M_\gamma=M_h=\xi p_T$, where ξ is a dimensionless scale factor. Unless stated otherwise, we put $\xi=1$ and employ the NLO set of the GRV photon PDF's [22] in the $\overline{\text{MS}}$ scheme. We take the NLO FF's for charged pions and kaons from our recent work [5]. We sum over charged charged pions and kaons. Charged-baryon production is likely to be negligible; in e^+e^- annihilation, some 10% of the charged tracks are due to protons and antiprotons [5], and one expects their fraction to be even smaller in $\gamma\gamma$ processes. In our MARK II analysis, we calculate the ratio of the K^0_S and charged-hadron cross sections. For this purpose, we employ the K^0_S FF's from our very recent work [6].

In the following three subsections, the results are ordered according to the various energy regions relevant for PETRA/PEP, LEP2, and NLC.

A. Results for PETRA/PEP energies

Before presenting our predictions at high energies (LEP2 and NLC), where we expect to see experimental data at large p_T in the near future, at least from LEP2, we wish to investigate how well the QCD-improved parton model can explain existing data at lower energies. Unfortunately, there are only few data for the inclusive cross section with information on the absolute normalization. Such data come from TASSO at PETRA [15] and MARK II at PEP [16]. In the TASSO experiment, the effective c.m. energy was $\sqrt{s}=33.1$ GeV, which is the average for runs with beam energies between 13.7 and 18.3 GeV [24]. The tagging requirements for the positrons and electrons were such that one of the two leptons (positron or electron) was tagged in the forward detector, which covered a narrow angular region between $\theta_{\min}=24$ mrad and $\theta_{\max}=60$ mrad relative to the beam direction, if it carried an energy of at least 4 GeV, whereas the other lepton (electron or positron) remained untagged [15]. In our theoretical evaluation, we take these tagging conditions into account by calculating the energy spectrum of the photons from the tagged leptons by means of the formula

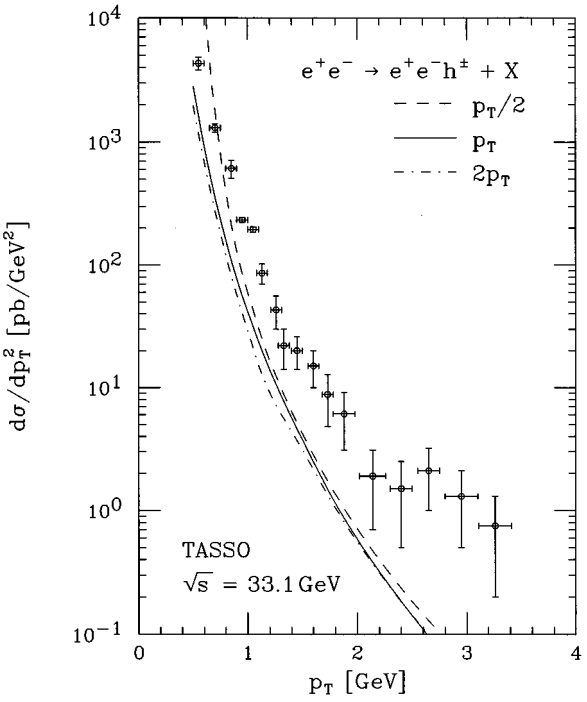

FIG. 1. Cross section $d\sigma/dp_T^2$ of inclusive charged-hadron production in single-tagged $\gamma\gamma$ collisions. The TASSO data [15] ($\sqrt{s}=33.1$ GeV on average) are compared with our corresponding NLO calculations for scale choices $\xi=1/2$, 1, and 2.

$$F_{\gamma/e}(x)=\frac{\alpha}{2\pi}\left[\frac{1+(1-x)^2}{x}\ln\frac{Q^2_{\max}}{Q^2_{\min}}+2m_e^2x\left(\frac{1}{Q^2_{\max}}-\frac{1}{Q^2_{\min}}\right)\right], \tag{7}$$

where m_e is the electron mass, $Q^2_{\min}=(1-x)E^2\theta^2_{\min}$, and similarly for $Q^2_{\max}$ ($E=\sqrt{s}/2$ is the beam energy). The tag-energy condition leads to a photon-energy cutoff at $x_{\max}=0.76$. The no-tag photon spectrum is calculated from the well-known formula by Brodsky *et al.* [25], written in a convenient form in Ref. [26]. Furthermore, we include an overall factor of 2 to account for the fact that both the positron and the electron can trigger the forward detector. The average Q^2 of the tagged photon was $\langle Q^2\rangle=0.35$ GeV^2 [15]. In our evaluation, we take $Q^2=0$ in the hard-scattering cross sections and photon PDF's. This is justified since $\langle Q^2\rangle \ll p_T^2$ for $p_T \gtrsim 2$ GeV, which we are primarily interested in. A further experimental constraint in the TASSO experiment was $|\cos\theta|<0.84$, where θ is the angle of charged tracks with respect to the beam axis [15]. This restricts the y range over which we integrate the doubly differential cross section $d^2\sigma/dy\,dp_T^2$ to be $|y|<1.22$. Taking these kinematical constraints into account, we calculate $d\sigma/dp_T^2$ for charged particles.

The result is shown in Fig. 1 as a function of p_T for the three different scale choices $\xi=1/2$, 1, and 2 and compared with the TASSO data. As we can see, the experimental cross section is systematically larger than the theoretical one. In particular at larger p_T, where our approach is supposed to be valid, the measurement greatly exceeds our prediction, even for $\xi=1/2$. At small p_T, we do expect that the data will overshoot our theoretical result, since in this region soft in-

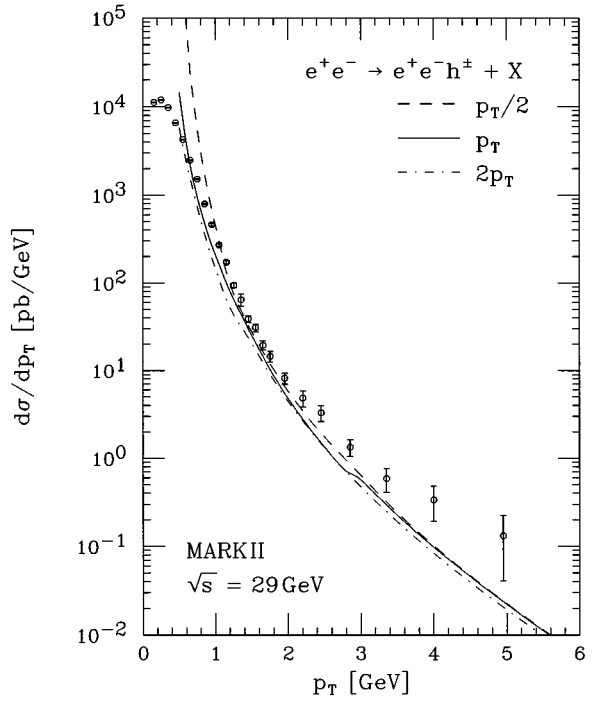

FIG. 2. Cross section $d\sigma/dp_T$ of inclusive charged-hadron production in single-tagged $\gamma\gamma$ collisions. The MARK II data [16] ($\sqrt{s}=29$ GeV) are compared with our corresponding NLO calculations for scale choices $\xi=1/2$, 1, and 2.

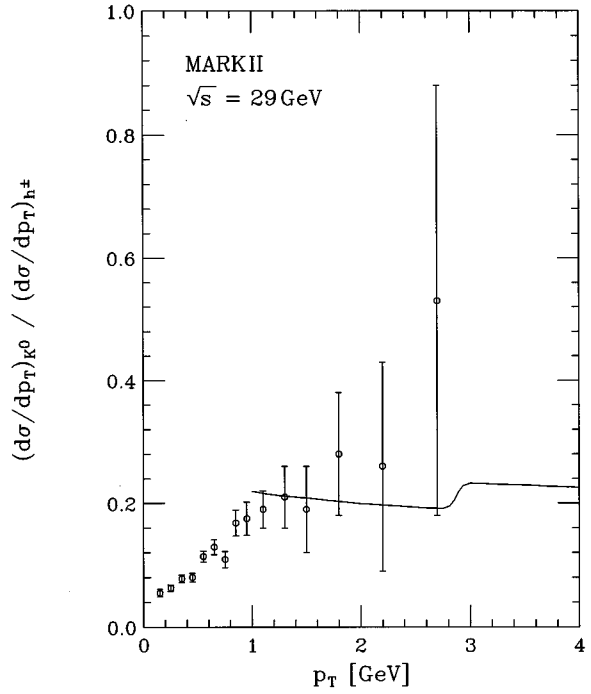

FIG. 3. The ratio of inclusive K_S^0 production to inclusive charged-hadron production as measured by MARK II [16] is compared with our NLO calculation for scale choice $\xi=1$. The rise near $p_T=3$ GeV is related to the c-quark threshold.

teractions give rise to additional particle production, which has not been subtracted from the data. This contribution is supposed to be significant for $p_T \lesssim 1.5$ GeV and is usually described as in hadronic reactions induced by the vector-dominance-mechanism (VDM) component of the photon. We have no explanation for the disagreement with the data in the upper p_T range. A serious background for the production of high-p_T events from one-photon annihilation events, where either of the incoming positron or electron radiates a hard photon, was thoroughly investigated by the TASSO Collaboration [15] and was subtracted from the data shown in Fig. 1. It is interesting to study the relative importance of the DD, DR, and RR contributions. At $p_T \lesssim 1$ GeV, the RR component is dominant, whereas for larger p_T the bulk of the cross section comes from the DD channel. At $p_T=(2, 3, 4)$ GeV, the DD component amounts to (51, 69, 75)%, respectively. This shows that, at these p_T values, the use of different photon PDF's would not change the cross section in any appreciable way and that the disagreement with the data is due to the DD component.

Single-tag measurements similar to those by TASSO were performed with the MARK II detector at PEP [16] operating with $\sqrt{s}=29$ GeV. The virtualities of the photons emitted from the tagged lepton were required to lie between $Q^2_{\rm min}=0.075$ GeV^2 and $Q^2_{\rm max}=1$ GeV^2 and had the average value $\langle Q^2\rangle=0.5$ GeV^2 [16]. The x range of these photons and the y range of the produced hadrons were only constrained by kinematics [16]. The MARK II data are confronted with our theoretical predictions for $\xi=1/2$, 1, and 2 in Fig. 2. The theoretical curves are multiplied by an overall factor of 1.2, to account for p_T smearing and resolution effects not corrected for in the experimental data [27]. We observe that the agreement between theory and experiment is considerably better than in the case of the TASSO data. At rather low p_T, where theory is not expected to be reliable because of the importance of the soft hadronic component, which was not subtracted in the data, there is almost perfect agreement, while the theoretical curves undershoot the data at large p_T. The dent at $p_T \approx 3$ GeV in the curve for $\xi=1$ is due to the onset of c-quark fragmentation [5]. The disagreement between the MARK II charged-particle cross section and the theoretical predictions at larger p_T has previously been noticed by Aurenche *et al.* [28] and by Gordon [14]. However, these authors used older FF's, partly in LO [28]. Our results, which are based on FF's that are rigorously constrained by recent e^+e^- data [5], suggest that this disagreement does not originate from the FF's. It also appears that, at large p_T, our results exceed those of Refs. [14,28].

The MARK II Collaboration also measured the cross section of inclusive K_S^0 production under kinematic constraints identical to those used for their charged-hadron sample [16]. Using our recently constructed set of K_S^0 FF's [6], we calculate the ratio of K_S^0 to charged-hadron production as a function of p_T. The results are compared with the MARK II data in Fig. 3, showing satisfactory agreement for $p_T \gtrsim 1$ GeV. The step in the theoretical curve at $p_T \approx 3$ GeV comes about because the c-quark threshold affects charged-hadron and K_S^0 production somewhat differently.

B. Results for LEP2

Unfortunately, there are no LEP1 data available which could be directly compared with our theoretical results. The ALEPH [29] and DELPHI [30] Collaborations reported on

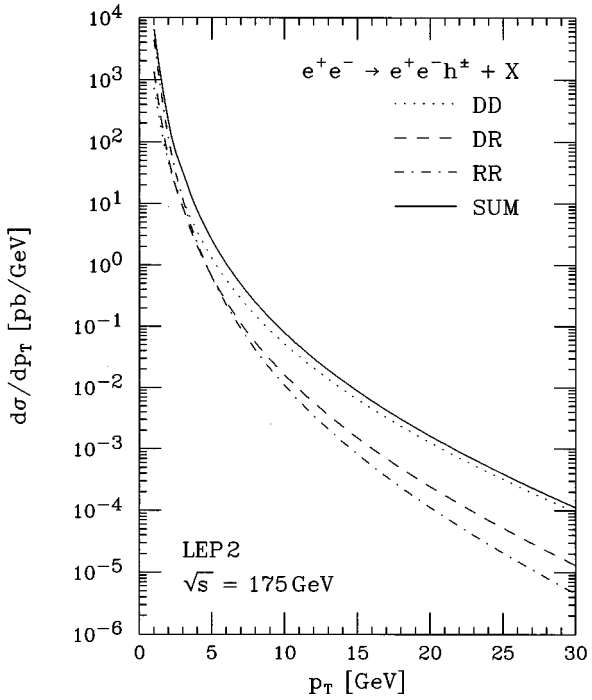

FIG. 4. NLO cross section $d\sigma/dp_T$ of inclusive charged-hadron production in double-tagged $\gamma\gamma$ collisions at LEP2 ($\sqrt{s}=175$ GeV). The DD, DR, and RR components are also shown.

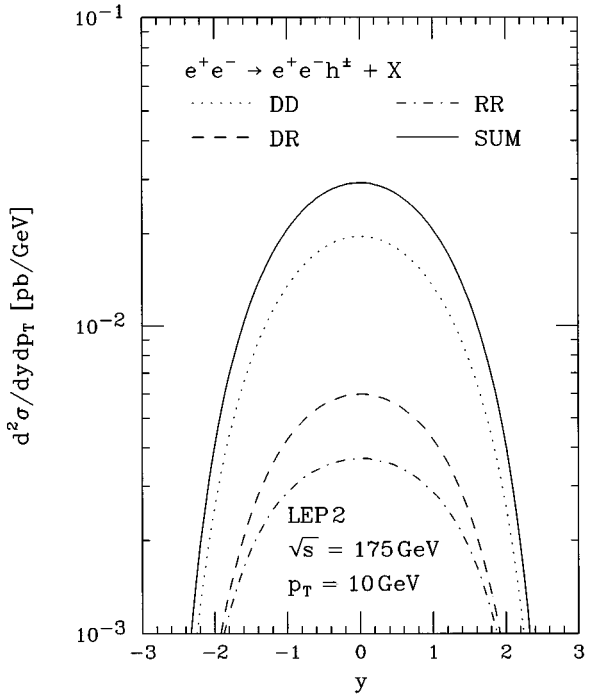

FIG. 5. Same as in Fig. 4 for the y dependence of $d^2\sigma/dy\ dp_T$ at $p_T=10$ GeV.

inclusive measurements of charged tracks, extending up to $p_T\approx 4$ GeV. However, these are not absolutely normalized, and the EPA constraints, which are indispensable for absolute predictions, are not specified.

It is hoped that better data, which extend to even larger p_T, will become available very soon from LEP2. For our predictions, we assume $\sqrt{s}=175$ GeV and describe the quasireal-photon spectrum in the EPA by the formula [31]

$$F_{\gamma/e}(x)=\frac{\alpha}{2\pi}\left\{\frac{1+(1-x)^2}{x}\ln\frac{E^2\theta_{\max}^2(1-x)^2+m_e^2x^2}{m_e^2x^2}+2(1-x)\left[\frac{m_e^2x}{E^2\theta_{\max}^2(1-x)^2+m_e^2x^2}-\frac{1}{x}\right]\right\}. \quad (8)$$

We vary $x=E_\gamma/E_e$ over the full range allowed by kinematics and put the antitagging angle to $\theta_{\max}=30$ mrad.

In Fig. 4, we show the DD, DR, and RR contributions to the cross section $d\sigma/dp_T$ of inclusive charged-hadron production and their sum as a function of p_T. As in the case of MARK II, $d\sigma/dp_T$ is obtained from $d^2\sigma/dy\ dp_T$ by integrating over the full y range. For $p_T\gtrsim 5$ GeV, the cross section is dominated by the DD component, which is then bigger than the sum of the DR and RR contributions. In general, the DR and RR components yield only a small fraction of the total sum, except for very small p_T ($p_T\lesssim 3$ GeV), where the RR part dominates. The y spectrum for $p_T=10$ GeV is plotted in Fig. 5, where the DD, DR, and RR contributions are again displayed along with their sum. Due to the symmetric experimental setup, the curves are symmetric in y. For $p_T=10$ GeV, the DD contribution dominates for all values of y. It is of interest to know whether the resolved contributions can be used to obtain information about the gluon PDF of the photon. Since for large p_T the DR and RR contributions are small, this should be feasible only for small p_T. To investigate this point, we repeat the computation of $d\sigma/dp_T$ putting $F_{g/\gamma}(x)=0$ and plot the ratio of the outcome to the full result in Fig. 6 (dashed line). We observe that this ratio is below

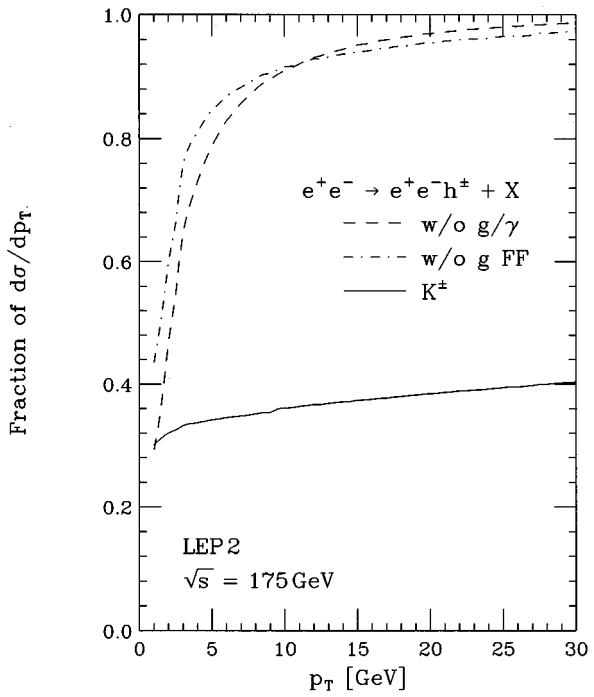

FIG. 6. Influence of the gluon PDF of the photon, the gluon FF, and the charged-kaon final states on the $\xi=1$ result of Fig. 4. Shown are the fractions that remain if the gluon is switched off in the photon PDF's (dashed line) or in the FF's (dot-dashed line) as well as the fraction due to charged-kaon production (solid line).

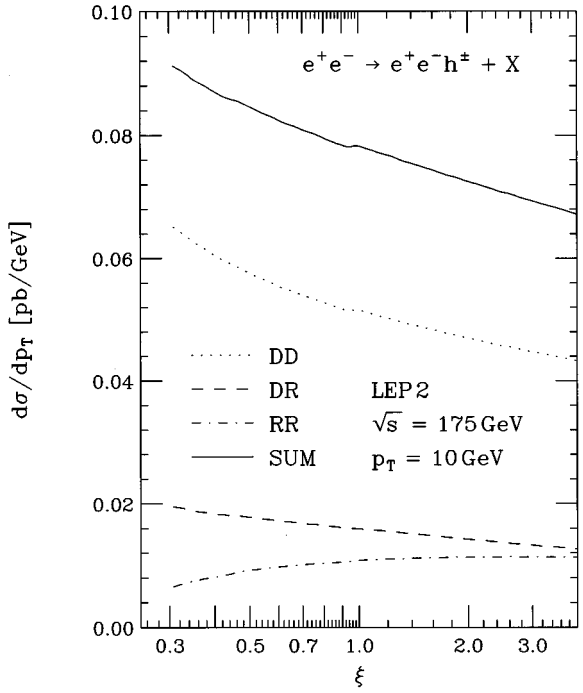

FIG. 7. ξ dependence of the results shown in Fig. 4 at $p_T=10$ GeV, in the interval $0.3<\xi<4$.

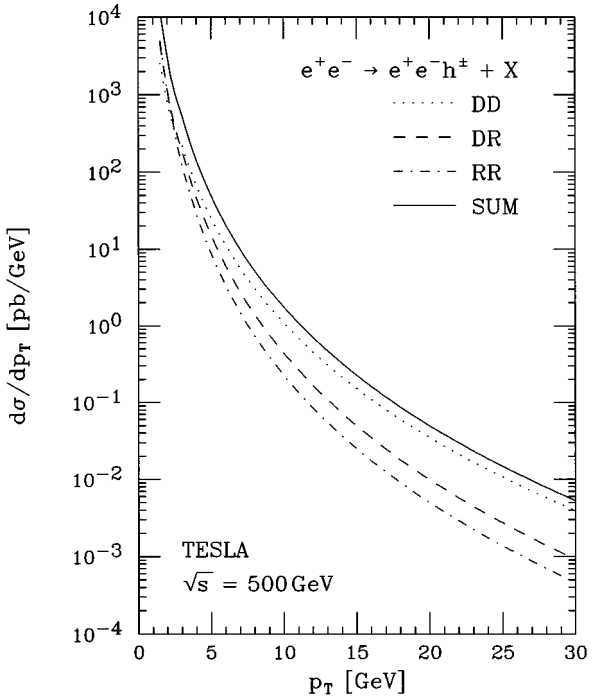

FIG. 8. Same as in Fig. 4 for the NLC with TESLA design ($\sqrt{s}=500$ GeV).

80% only if $p_T \lesssim 5$ GeV. This means that this cross section is not a very powerful discriminator to disentangle the gluon PDF of the photon. Almost the same pattern is observed if the gluon FF is switched off (dot-dashed line). The cross section $d\sigma/dp_T$ is sensitive to $D_{h^\pm/g}(x)$ only for small p_T. This may be understood by observing that the gluon FF falls off much more rapidly with increasing x than the quark FF's. In Fig. 6, we also show the fraction of $d\sigma/dp_T$ originating from the fragmentation into $K^\pm$. It is rather large, ranging between 34% and 40% for p_T between 5 and 30 GeV.

It is generally believed that the scale dependence of a parton-model calculation to a given order indicates the size of unknown higher-order corrections and thus may be used to estimate the theoretical uncertainty of the prediction. This leads us to study in Fig. 7 the ξ dependence of $d\sigma/dp_T$ and its DD, DR, and RR parts for $p_T=10$ GeV. This scale dependence is determined mostly by the DD component, which dominates the cross section at $p_T=10$ GeV. In the range $1/2<\xi<2$, the total sum varies by $\pm 8\%$ relative to its value at $\xi=1$. The discontinuity at $\xi=0.95$ stems from the b-quark threshold.

C. Results for NLC

Next, we consider the predictions for the NLC with $\sqrt{s}=500$ GeV and TESLA design. At the NLC, photons are produced not only by bremsstrahlung, but also via synchrotron radiation emitted by one of the colliding bunches in the field of the opposing bunch [32]. This phenomenon has been termed beamstrahlung. The details of the beamstrahlung spectrum depend crucially on the design and operation mode of the NLC. In our study, we select the TESLA design, where the unwanted effects of beamstrahlung are reduced to a tolerable level. We coherently superimpose the EPA and beamstrahlung spectra. The EPA spectrum is computed from Eq. (8) with $\theta_{\max}=175$ mrad and the beamstrahlung spectrum from the expression given in Ref. [32], with parameters $\Upsilon_{\rm eff}=0.039$ and $\sigma_2=0.5$ mm [33]. This combined spectrum has recently been used also in a study of heavy-quark production in $\gamma\gamma$ collisions [34]. The p_T distribution, integrated over the full y range, is shown in Fig. 8 together with its DD, DR, and RR components. Apart from an overall enhancement due to the increased EPA logarithm and the additional beamstrahlung-induced contribution, the p_T spectrum looks very similar to the LEP2 case in Fig. 4. The corresponding y spectra for $p_T=10$ GeV are shown in Fig. 9. Due to the admixture of beamstrahlung, their shapes differ somewhat from those of the pure EPA case in Fig. 5.

The highest possible photon energies with large enough luminosity may be achieved by converting the NLC into a $\gamma\gamma$ collider via backscattering of high-energetic laser light off the e^+ and e^- beams [35]. The resulting photon spectrum is given by [35]

$$F_\gamma(x)=\frac{1}{G(\kappa)}\left[1-x+\frac{1}{1-x}-\frac{4x}{\kappa(1-x)}+\frac{4x^2}{\kappa^2(1-x)^2}\right], \tag{9}$$

where

$$G(\kappa)=\left(1-\frac{4}{\kappa}-\frac{8}{\kappa^2}\right)\ln(1+\kappa)+\frac{1}{2}+\frac{8}{\kappa}-\frac{1}{2(1+\kappa)^2}. \tag{10}$$

This spectrum extends up to $x_{\max}=\kappa/(1+\kappa)$. In our calculation we chose $\kappa=4.83$, so that $x_{\max}=0.83$. If the experimental setup was arranged so that $\kappa>4.83$, e^+e^- pairs would be produced in the collisions of the primary laser photons and the high-energetic backscattered photons. In

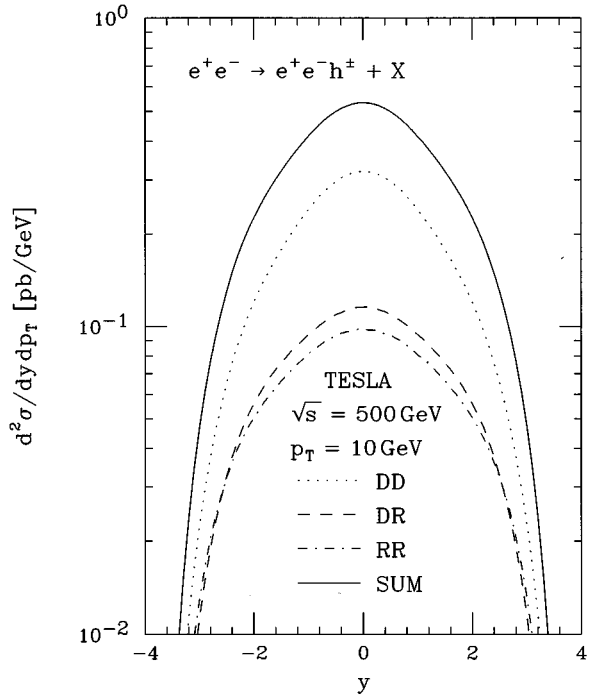

FIG. 9. Same as in Fig. 5 for the NLC with TESLA design ($\sqrt{s}=500$ GeV).

Fig. 10, we present the DD, DR, and RR contributions to the p_T spectrum $d\sigma/dp_T$ together with their sum. Compared to the previous cases, the relative magnitudes of the DD, DR, and RR components have completely changed. At small p_T, at about 5 GeV say, the RR component is by far the largest, whereas the DD component is negligible. At large p_T, around 20 GeV, the relation is quite different; the DD,

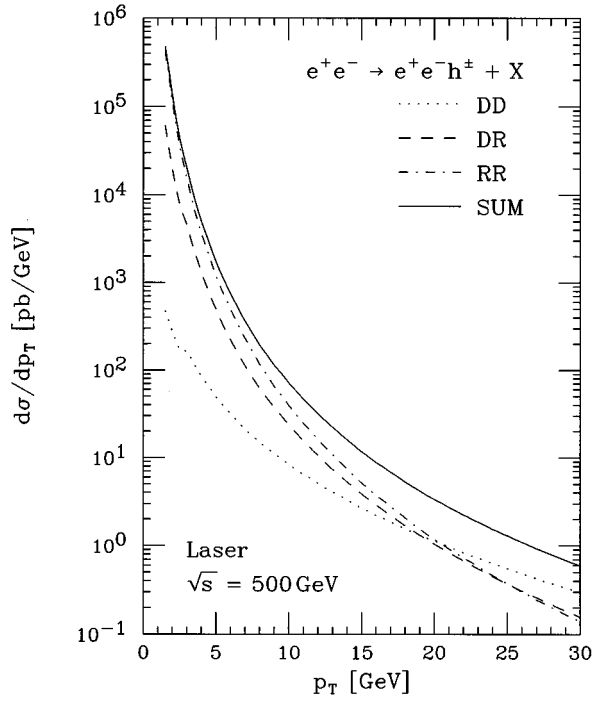

FIG. 10. Same as in Fig. 4 for the NLC in the Compton-backscattering mode ($\sqrt{s}=500$ GeV).

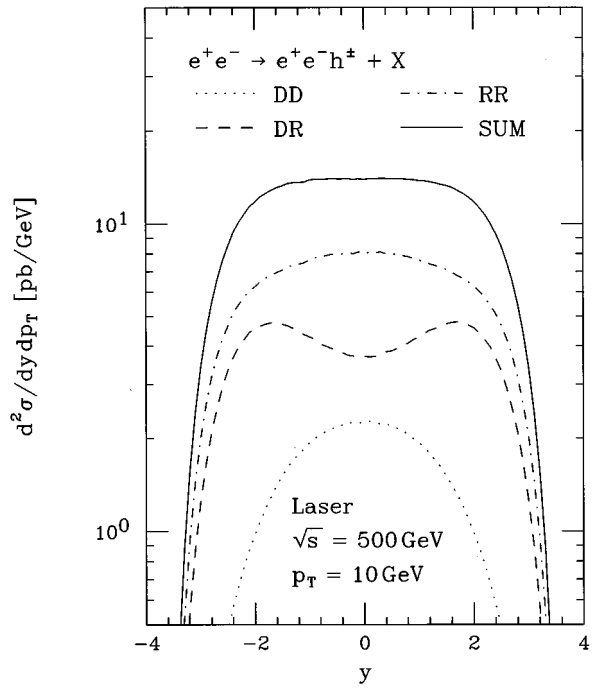

FIG. 11. Same as in Fig. 5 for the NLC in the Compton-backscattering mode ($\sqrt{s}=500$ GeV).

DR, and RR contributions all have the same order of magnitude. A similar situation was encountered in the analogous study of heavy-quark production [34]. Consequently, in the lower p_T range, the cross section $d\sigma/dp_T$ of inclusive particle production with a Compton collider will serve as a powerful tool to extract information on the photon PDF's. The corresponding y spectra for $p_T=10$ GeV are plotted in Fig. 11. As far as the relative importance of the various components is concerned, we recognize a pattern similar to Fig. 10, which refers to the integrated rapidity spectrum, at $p_T=10$ GeV. On the other hand, the y spectra are quite different in shape and relative magnitude from those found in the TESLA case. This may be understood by observing that the laser-photon spectrum is peaked at the upper edge. The RR component is now dominant and rather flat; the DR component is somewhat smaller and exhibits a characteristic two-hump structure with a significant depletion in the central region; the DD component is greatly suppressed, but exhibits a shape similar to the TESLA case. As a consequence, there is a pronounced plateau in the y spectrum of the total sum. Inspired by the observations made in Fig. 10, we quantitatively study in Fig. 12 the influence of the gluon PDF of the photon. The dashed line represents the ratio of $d\sigma/dp_T$ with the gluon PDF switched off to the full result as a function of p_T. We see that, at $p_T=(5, 15, 25)$ GeV, (75, 42, 23)% of the cross section stems from the gluon PDF. The NLO photon PDF set by Gordon and Storrow (GS) [36] differs from the GRV set [22] mainly in the gluon PDF. The ratio of $d\sigma/dp_T$ evaluated with the GS set to the GRV result is visualized in Fig. 12 by the solid line, which is a smooth interpolation. Obviously, the GS and GRV predictions appreciably differ at small p_T, by up to a factor of 2. Thus the NLC operated as a $\gamma\gamma$ collider would provide an excellent laboratory to pin down the poorly known gluon PDF of the photon. In Fig. 12, we also assess the sensitivity of such an

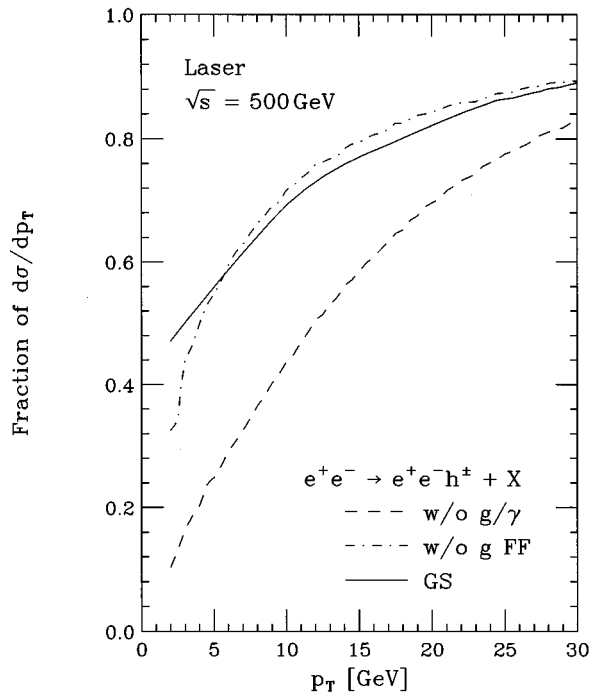

FIG. 12. Influence of the gluon PDF of the photon and the gluon FF on the total result of Fig. 10. Shown are the fractions that remain if the gluon is switched off in the photon PDF's (dashed line) or in the FF's (dot-dashed line) as well as the ratio of the calculation with the GS photon PDF's to that with the GRV set (solid line). The solid line is a smooth interpolation.

experiment to the gluon FF by showing the fraction of $d\sigma/dp_T$ due to the quark FF's (dot-dashed line). At $p_T=(5, 15, 25)$ GeV, (45, 21, 13)% of the cross section is related to gluon fragmentation. Consequently, the $\gamma\gamma$ NLC would also allow one to probe the gluon FF, which is only moderately constrained by data of inclusive hadron production via e^+e^- annihilation.

IV. SUMMARY AND CONCLUSIONS

We studied the inclusive production of charged hadrons in collisions of almost real photons at NLO in the framework of the QCD-improved parton model. This approach is conceptually very different from the one based on MC event generators, which is frequently followed by experimentalists to interpret their data. In these MC programs, the various QCD processes are simulated using LO matrix elements in connection with certain model assumptions concerning the formation of hadronic final states. Although these MC packages often lead to satisfactory descriptions of the data, from the theoretical point of view, their drawback is that this happens at the expense of introducing a number of *ad hoc* fine-tuning parameters, which do not originate in the QCD Lagrangian. Furthermore, in the MC approach, it seems impossible to implement the factorization of final-state collinear singularities, which impedes a consistent extension to NLO. On the contrary, in the QCD-improved parton model, such singularities are absorbed into the bare (infinite) FF's so as to render them renormalized (finite) in a way quite similar to the procedure for the PDF's at the incoming legs. In our analysis, we used FF's extracted with NLO precision from PEP and recent LEP1 data on inclusive single-hadron production in e^+e^- annihilation [5,6]. In fact, owing to the factorization theorem [1], the FF's are process independent as long as one considers unbiased single-hadron event samples. By the same token, our formalism is less flexible than the MC approach, since we are unable to describe more complicated final states, with more than one detected hadron and acceptance cuts on observables different from our integration variables.

There are various ways to realize $\gamma\gamma$ processes in experiments. The conventional method is to exploit the QED bremsstrahlung which is radiated during e^+e^- reactions from the colliding beams. High-quality data of this type were collected by TASSO [15] at PETRA and MARK II [16] at PEP. Unfortunately, the bulk of these data are accumulated at rather small p_T, where the NLO formalism is not expected to yield reliable results, and the few data points at larger p_T values carry considerable error bars due to limited statistics. Detailed comparison revealed that our consistent NLO calculation with up-to-date FF's was able to reduce somewhat the mismatch between theory and experiment that had previously been observed by other authors [14,28]. However, especially in the case of TASSO, the degree of discrepancy in the upper p_T range still gives some reason for concern.

While at LEP1 the $\gamma\gamma$ processes were overwhelmed beneath the tremendous background due to e^+e^- annihilation on the Z resonance, the situation will be much more favorable at LEP2. We presented NLO predictions for the p_T and y spectra to be measured in the oncoming LEP2 phase. We verified that our NLO predictions are rather stable under scale variations; at $p_T=10$ GeV, the cross section only fluctuates by $\pm 8\%$ if ξ is varied between 1/2 and 2. Unfortunately, except at rather low p_T, the study of $\gamma\gamma$ processes at LEP2 will not much deepen our understanding of the nature of the gluon inside the photon and of its role within the fragmentation process.

Photon-photon physics at the NLC will greatly benefit from beamstrahlung as an additional source of quasireal photons and, of course, from the increased EPA logarithm. In the case of the 500-GeV NLC with TESLA architecture, the cross sections at $p_T=(5, 15, 25)$ GeV exceed the corresponding LEP2 values by factors of (19, 26, 37), respectively, while the shapes of the p_T and y spectra closely resemble their LEP2 counterparts.

The advent of a Compton collider, generated by backscattering of laser light off the e^+ and e^- beams of the NLC, would represent an important step forward in the history of $\gamma\gamma$ experimentation, and might considerably improve our knowledge of both the gluon FF and the gluon PDF of the photon. By converting the NLC, the cross sections of inclusive charged-hadron production at $p_T=(5, 15, 25)$ GeV would be increased by factors of (35, 52, 88), respectively. At the same time, the relative importance of the DD channel would be dramatically reduced, so that the sensitivity to the photon PDF's would be correspondingly amplified.

ACKNOWLEDGMENTS

We thank E. Hilger and N. Wermes for very useful communications concerning Ref. [15], G. Gidal for drawing our attention to Ref. [27], and L.E. Gordon for providing us with

the FORTRAN implementation of his NLO results for the DD channel [14]. One of us (G.K.) is grateful to the Theory Group of the Werner-Heisenberg-Institut for the hospitality extended to him during a visit when this paper was prepared. This work was supported by Bundesministerium für Forschung und Technologie, Bonn, Germany, under Contract No. 05 6 HH 93P (5), and by EEC Program ''Human Capital and Mobility'' through Network ''Physics at High Energy Colliders'' under Contract No. CHRX-CT93-0357 (DG12 COMA).

[1] H.D. Politzer, Phys. Rev. Lett. **30**, 1346 (1973); Phys. Lett. **70B**, 430 (1977); R.K. Ellis, H. Georgi, M. Machacek, H.D. Politzer, and G.G. Ross, *ibid.* **78B**, 281 (1978); Nucl. Phys. **B152**, 285 (1979).

[2] R. Baier, J. Engels, and B. Petersson, Z. Phys. C **2**, 265 (1979); M. Anselmino, P. Kroll, and E. Leader, *ibid.* **18**, 307 (1983).

[3] P. Chiappetta, M. Greco, J.-Ph. Guillet, S. Rolli, and M. Werlen, Nucl. Phys. **B412**, 3 (1994); M. Greco and S. Rolli, Z. Phys. C **60**, 169 (1993); Phys. Rev. D **52**, 3853 (1995); M. Greco, S. Rolli, and A. Vicini, Z. Phys. C **65**, 277 (1995).

[4] J. Binnewies, B.A. Kniehl, and G. Kramer, Z. Phys. C **65**, 471 (1995).

[5] J. Binnewies, B.A. Kniehl, and G. Kramer, Phys. Rev. D **52**, 4947 (1995).

[6] J. Binnewies, B.A. Kniehl, and G. Kramer, Phys. Rev. D **53**, 3573 (1996).

[7] G.D. Cowan, in *Proceedings of the XXVII International Conference on High Energy Physics*, Glasgow, Scotland, 1994, edited by P. Bussey and I. Knowles (World Scientific, Singapore, 1995); and private communication; C. Padilla Aranda (private communication).

[8] ALEPH Collaboration, D. Buskulic *et al.*, Phys. Lett. B **357**, 487 (1995); **364**, 247(E) (1995); C. Padilla Aranda, Ph.D. thesis, University of Barcelona, 1995.

[9] V.N. Gribov and L.N. Lipatov, Yad. Fiz. **15**, 781 (1972) [Sov. J. Nucl. Phys. **15**, 438 (1972)]; G. Altarelli and G. Parisi, Nucl. Phys. **B126**, 298 (1977); Yu.L. Dokshitser, Zh. Éksp. Teor. Fiz. **73**, 1216 (1977) [Sov. Phys. JETP **46**, 641 (1977)].

[10] H1 Collaboration, I. Abt *et al.*, Phys. Lett. B **328**, 176 (1994); M. Erdmann, K. Johannsen, and F. Linsel (private communications).

[11] ZEUS Collaboration, M. Derrick *et al.*, Z. Phys. C **67**, 227 (1995).

[12] UA1 Collaboration, G. Bocquet *et al.*, Phys. Lett. B **366**, 434 (1996); **366**, 441 (1996); H. Dibon (private communication).

[13] F.M. Borzumati and G. Kramer, Z. Phys. C **67**, 137 (1995).

[14] L.E. Gordon, Phys. Rev. D **50**, 6753 (1994).

[15] TASSO Collaboration, R. Brandelik *et al.*, Phys. Lett. **107B**, 290 (1981); N. Wermes, Ph.D. thesis, Bonn University Report No. BONN-IR-82-27, 1982 (unpublished); and private communication.

[16] MARK II Collaboration, D. Cords *et al.*, Phys. Lett. B **302**, 341 (1993).

[17] M. Drees and R.M. Godbole, Nucl. Phys. **B339**, 355 (1990).

[18] P. Aurenche, R. Baier, A. Douiri, M. Fontannaz, and D. Schiff, Z. Phys. C **29**, 423 (1985).

[19] P. Aurenche, R. Baier, A. Douiri, M. Fontannaz, and D. Schiff, Nucl. Phys. **B286**, 553 (1987).

[20] F. Aversa, P. Chiappetta, M. Greco, and J.-Ph. Guillet, Nucl. Phys. **B327**, 105 (1989).

[21] F.M. Borzumati, B.A. Kniehl, and G. Kramer, Z. Phys. C **59**, 341 (1993); B.A. Kniehl and G. Kramer, Z. Phys. C **62**, 53 (1994); B.A. Kniehl, in *Proceedings of the Workshop on Two-Photon Physics at LEP and HERA*, Lund, Sweden, 1994, edited by G. Jarlskog and L. Jönsson (Krontryck, Eslöv, 1994), p. 264.

[22] M. Glück, E. Reya, and A. Vogt, Phys. Rev. D **46**, 1973 (1992).

[23] M. Drees and R.M. Godbole, Z. Phys. C **59**, 591 (1993).

[24] E. Hilger (private communication).

[25] S.J. Brodsky, T. Kinoshita, and H. Terazawa, Phys. Rev. D **4**, 1532 (1971).

[26] B.A. Kniehl, Phys. Lett. B **254**, 267 (1991); P. Aurenche, J.-Ph. Guillet, M. Fontannaz, Y. Shimizu, J. Fujimoto, and K. Kato, Prog. Theor. Phys. **92**, 175 (1994).

[27] G. Gidal, in *Proceedings of the VIIth International Workshop on Photon-Photon Collisions*, Paris, France, 1986, edited by A. Courau and P. Kessler (World Scientific, Singapore, 1986), p. 418; and private communication.

[28] P. Aurenche, J.-Ph. Guillet, M. Fontannaz, Y. Shimizu, and K. Kato, in *Proceedings of the Workshop on Two-Photon Physics at LEP and HERA*, Lund, Sweden, 1994 [21], p. 269.

[29] ALEPH Collaboration, D. Buskulic *et al.*, Phys. Lett. B **313**, 509 (1993); A.J. Finch (private communication).

[30] DELPHI Collaboration, P. Abreu *et al.*, Z. Phys. C **62**, 357 (1994).

[31] S. Frixione, M.L. Mangano, P. Nason, and G. Ridolfi, Phys. Lett. B **319**, 339 (1993).

[32] T. Barklow, P. Chen, and W. Kozanecki, in Proceedings of the Workshop on e^+e^- Collisions at 500 GeV: The Physics Potential, edited by P.M. Zerwas, DESY Orange Report No. 92-123B, 1992 (unpublished), p. 845; P. Chen, T.L. Barklow, and M.E. Peskin, Phys. Rev. D **49**, 3209 (1994).

[33] D. Schulte (private communication).

[34] M. Cacciari, M. Greco, B.A. Kniehl, M. Krämer, G. Kramer, and M. Spira, Report Nos. DESY 95-205, FNT/T-95/28, LNF-95/059(P), MPI/PhT/95-113, and hep-ph/9512246, 1995 [Nucl. Phys. B (to be published)].

[35] I.F. Ginzburg, G.L. Kotkin, S.L. Panfil, V.G. Serbo, and V.I. Telnov, Nucl. Instrum. Methods **219**, 5 (1984).

[36] L.E. Gordon and J.K. Storrow, Z. Phys. C **56**, 307 (1992).